2017 American Control Conference
Sheraton Seattle Hotel
May 24–26, 2017, Seattle, USA

Time-dependent Orbital Stabilization of Underactuated Bipedal Walking

Yan Gu, Bin Yao, and C. S. George Lee †

Abstract— **In this paper, we propose to study the orbitally exponential stabilization of underactuated bipedal robotic walking with an impulse effect through time-dependent output feedback control. In gait characterization, symmetric periodic gaits are considered and defined. Input-output linearization is then utilized to synthesize an output feedback controller, which drives the directly controlled joints to track some desired time functions that are defined based on the desired periodic symmetric gait. Due to the underactuation, nonautonomous internal dynamics exists and determines the closed-loop stability of the control system. By introducing a new state, the nonautonomous closed-loop system can be transformed into an equivalent autonomous system with an augmented set of states. Stability conditions of the original nonautonomous closed-loop system are then established based on the stability analysis of the equivalent autonomous system. Finally, simulation results showed that the proposed time-dependent output feedback control can indeed realize orbitally exponential stabilization of underactuated bipedal robotic walking if the proposed stability conditions are satisfied.**

I. INTRODUCTION

There are multiple approaches to solving the challenging problem of stabilizing bipedal robotic walking, among which the most extensively studied one is based on the concept of Zero Moment Point (ZMP). If the ZMP is kept strictly within the support polygon, the support foot will remain in full contact with the ground and thus tipping over around the foot edge can be avoided [1] [2] [3]. Disadvantages of the ZMP-based approach include high energy consumption and conservative walking speeds.

Instead of focusing on a specific ground-reference point, previous studies on underactuated bipedal walking achieve walking stabilization by orbitally stabilizing the closed-loop system based on nonlinear control theories [4] [5]. Virtual constraints are introduced as the desired walking pattern, which defines the desired relative evolution of the directly controlled joints with respect to a parameterization variable and is enforced through output feedback control. The paramerization variable can be chosen as joint position [4], angular momentum [6], or joint velocity [7]. If there is only one degree of underactuation and the desired walking pattern is designed properly, hybrid zero dynamics (HZD) exists; that is, the continuous-phase zero dynamics will be invariant with respect to a landing impact [8]. For higher degrees of underactuation, HZD exists if the definitions of output functions are updated each time upon an impact [9]. Stability of the autonomous HZD can be conveniently evaluated numerically, and it indicates the stability of the original closed-loop system, which significantly reduces the dimension of stability analysis [9]. Specifically, if there exists an exponentially stable orbit in the hybrid invariance manifold and if the convergence rate to the hybrid invariance manifold is sufficiently fast, then the closed-loop system is orbitally exponentially stable. In comparison with the ZMP-based approach, faster walking speed and higher energy efficiency are inherent features associated with the orbital stabilization approach.

In the above-mentioned previous work on orbital stabilization, the virtual constraints are defined as functions of states (i.e., joint position, angular momentum, and joint velocity) alone. When some of the virtual constraints are defined as explicit functions of time, implementation issues caused by sensor noise, which is associated with the state-based approach, can be effectively solved [10]. However, the resulting closed-loop system becomes nonautonomous, and its stability is not straightforward to evaluate. Time-dependent orbital stabilization of underactuated walking was previously investigated, but no sufficient conditions for orbitally exponential stabilization were provided [10] [11]. This study focuses on orbitally exponential stabilization of underactuated bipedal walking based on time-dependent output feedback control. During the continuous phases, the directly controlled joints of a biped are driven to follow some desired time functions, which are defined base on the planned periodic gait, and all of the joints will converge to the corresponding periodic orbit exponentially fast if the proposed stability conditions are satisfied.

In Section II, we present the problem formulation including dynamic modeling, gait definition, and output feedback control. The main theorem is introduced in Section III, which provides sufficient conditions for orbitally exponential stabilization. A planar biped with five revolute joints and point feet is simulated to show the validity of the proposed walking strategy in Section IV.

II. PROBLEM FORMULATION

The main objective of this study is to achieve orbitally exponential stabilization of underactuated bipedal walking through time-dependent output feedback control. The walking process is modeled as a hybrid dynamical system with impulsive landing impacts, and the desired time functions to be tracked are defined based on the modification of the desired periodic symmetric gait. Output feedback control is

†Yan Gu and Bin Yao are with the School of Mechanical Engineering, and C. S. George Lee is with the School of Electrical and Computer Engineering, Purdue University, West Lafayette, IN 47907, U.S.A. Email: {gu49, byao, csglee}@purdue.edu. Bin Yao, the corresponding author, is also a Chang-Jiang Chair Professor at Zhejiang University, China.

This work was supported in part by the National Science Foundation under Grant IIS-0916807. Any opinion, findings, and conclusions or recommendations expressed in this material are those of the authors and do not necessarily reflect the views of the National Science Foundation.

then utilized to drive the directly controlled joints to follow the desired time functions exponentially fast during each continuous phase. However, due to the underactuation, the closed-loop system is not necessarily stable under such a control law without satisfying additional conditions. Based on the problem formulation in this section, conditions for the closed-loop stability will be introduced in Section III.

A. Hybrid Dynamics of Bipedal Walking

Similar to previous studies, the double-support phase during walking is assumed to be instantaneous, and the swing-foot landing is modeled as a rigid impact of an infinitesimal period of time [4] [5] [12]. Suppose that the ground-contact constraints are satisfied including the friction cone and the unilateral constraints, dynamics of bipedal walking on an even flat terrain can be written as:

$$\begin{cases} \mathbf{M}(\mathbf{q})\ddot{\mathbf{q}}+\mathbf{h}(\mathbf{q},\dot{\mathbf{q}}) = \mathbf{B}_u\mathbf{u}, & \text{if } \mathbf{q} \notin S_q(\mathbf{q},\dot{\mathbf{q}}); \\ [\boldsymbol{\Delta}\mathbf{q}^T, \boldsymbol{\Delta}\dot{\mathbf{q}}^T]^T = \mathbf{I}_q(\mathbf{q},\dot{\mathbf{q}}), & \text{if } \mathbf{q} \in S_q(\mathbf{q},\dot{\mathbf{q}}); \end{cases} \tag{1}$$

where $\mathbf{q}$, $\dot{\mathbf{q}}$, $\ddot{\mathbf{q}} \in \mathbb{R}^n$ represent the joint positions, velocities, and accelerations, respectively, $\mathbf{M}(\mathbf{q}) \in \mathbb{R}^{n\times n}$ is the inertia matrix, $\mathbf{h}(\mathbf{q},\dot{\mathbf{q}}) \in \mathbb{R}^n$ is the sum of Coriolis, centrifugal, and gravitational terms, $\mathbf{u} \in \mathbb{R}^{n\times m}$ $(n > m)$ is the joint-torque vector, $\mathbf{B}_u \in \mathbb{R}^{n\times n}$ is the input matrix, $S_q(\mathbf{q},\dot{\mathbf{q}})$ is the switching surface, $\boldsymbol{\Delta}\mathbf{q}(t) = \mathbf{q}(t^+) - \mathbf{q}(t^-)$, $\boldsymbol{\Delta}\dot{\mathbf{q}}(t) = \dot{\mathbf{q}}(t^+) - \dot{\mathbf{q}}(t^-)$, and $\mathbf{I}_q(\mathbf{q},\dot{\mathbf{q}}) \in \mathbb{R}^n$ represents the reset map determined by a rigid impact with an impulse effect and the coordinate swap. Here, left continuity at an impact is assumed and $\mathbf{q}(t) = \mathbf{q}(t^-)$. The switching surface $S_q(\mathbf{q},\dot{\mathbf{q}})$, which determines the moments of swing-foot landings, is defined as

$$S_q(\mathbf{q},\dot{\mathbf{q}}) := \{\mathbf{q},\dot{\mathbf{q}} \in \mathbb{R}^n : \mathrm{h}(\mathbf{q}) = 0, \frac{\partial \mathrm{h}}{\partial \mathbf{q}}\dot{\mathbf{q}} < 0\}, \tag{2}$$

where $h(\mathbf{q})$ represents the swing-foot height.

Consider a planar bipedal robot in the sagittal plane (see Fig. 1). The biped has point feet and five revolute joints. The masses are assumed to be lumped at the center of each link. The two legs are identical. The lengths of the lower limbs, the upper limbs, and the trunk are l_1, l_2, and r, respectively. Denote

$$\mathbf{q} = [q_1, q_2, q_3, q_4, q_5]^T \in \mathbb{R}^5,$$

where q_1 and q_5 represent the lower-limb joint positions of the support and the swing legs, respectively, q_2 and q_4 represent the upper-limb joint positions of the support and the swing legs, respectively, and q_3 represents the trunk joint position.

As illustrated in Fig. 1, there are four actuators, one at each knee and two at the hip. Denote

$$\mathbf{u} = [u_1, u_2, u_3, u_4]^T \in \mathbb{R}^4.$$

During the continuous phase, which is the single-support phase (SSP), there is only one foot touching the ground, and thus the biped has five degrees of freedom (DOF). The biped is considered underactuated because only four of its five joints can be directly controlled. Without loss of generality, the lower limb of the support leg, q_1, is chosen to be not directly controlled. Let

$$\mathbf{q}_a := [q_2, q_3, q_4, q_5]^T \in \mathbb{R}^4$$

denote the directly controlled joints.

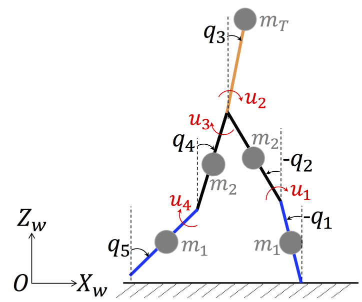

Fig. 1. A planar biped in the sagittal plane. Lumped masses: $m_1 = 3\ kg$, $m_2 = 6\ kg$, $m_T = 20\ kg$. Link lengths: $l_1 = l_2 = r/2 = 0.4\ m$.

B. A Periodic Symmetric Gait

Before the controller design is introduced, the desired periodic symmetric gait to be tracked is described, which corresponds to a periodic orbit in the state space. A symmetric gait can be conveniently characterized by the support and the swing legs, while an asymmetric gait can be more conveniently characterized by the left and the right legs [13]. Since this paper focuses on controller design and stability analysis, only symmetric gaits, which are characterized by the support and the swing legs, are considered. However, the results of this study can be readily extended to asymmetric gaits.

Let $\tau > 0$ denote the time between two successive swing-foot landings of a periodic symmetric gait. Then, τ is the least gait cycle. Let $\bar{\mathbf{q}}_d(t)$ denote the joint trajectories generated by the desired periodic symmetric gait with the initial condition $[\bar{\mathbf{q}}_d^T(0), \dot{\bar{\mathbf{q}}}_d^T(0)]^T$:

$$\bar{\mathbf{q}}_d(t) := [\bar{q}_{1d}(t), \bar{q}_{2d}(t), \bar{q}_{3d}(t), \bar{q}_{4d}(t), \bar{q}_{5d}(t)]^T \tag{3}$$

$$:= \begin{bmatrix} \bar{q}_{1d}(t) \\ \bar{\mathbf{q}}_{ad}(t) \end{bmatrix}. \tag{4}$$

An example of the lower-limb joint trajectories $\bar{q}_{1d}(t)$ and $\bar{q}_{5d}(t)$ is illustrated in Fig. 2.

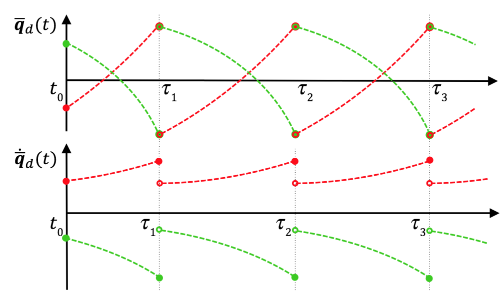

Fig. 2. An illustration of $\bar{\mathbf{q}}_d(t)$ and $\dot{\bar{\mathbf{q}}}_d(t)$. Red: the support-leg lower limb angle $\bar{q}_{1d}(t)$. Green: the swing-leg lower limb angle $\bar{q}_{5d}(t)$.

Note that

$$\bar{\mathbf{q}}_d(t) = \bar{\mathbf{q}}_d(t + k\tau),\ t > t_0, \tag{5}$$

with discontinuities caused by the swing-foot landing at $t = \tau_k := \tau_1 + (k-1)\tau$, where $\tau_k > t_0$ $(k \in \{1, 2, ...\})$ represents the k^{th} moment of swing-foot landing. Without loss of generality, assume $\tau_0 = t_0 = 0$, and thus $\tau_k = k\tau$ for $k \in$

$\{0,1,2,...\}$. Both joint positions and velocities experience a sudden jump upon a swing-foot landing due to the coordinate swap and the rigid impact with an impulse effect.

C. Output Feedback Control

In previous related studies on controlling underactuated bipedal walking [4], the desired walking pattern is chosen to be tracked through output feedback control. Since a walking pattern is defined as a function of states alone, the resulting closed-loop system is autonomous, and the walking can be orbitally (exponentially) stabilized [14]. Here, we want to orbitally stabilize the walking process through time-dependent output feedback control. This problem is challenging partly due to the underactuation and the nonautonomous hybrid dynamics with internal dynamics. In this study, an output feedback controller is designed to directly drive the actuated joints $\mathbf{q}_a(t)$ to follow some desired time functions during each continuous phase. The unactuated joint $q_1(t)$ will automatically converge to the desired orbit exponentially fast if certain stability conditions, which will be introduced in the next section, are met.

Because the support and the swing legs switch their roles at the landing events during walking, the desired time functions $\mathbf{q}_d(t)$ that are used to define the output functions should be accordingly updated upon swing-foot landings. During the $(k+1)^{th}$ step, $k \in \{0,1,2,...\}$, the desired time functions $\mathbf{q}_d(t)$ are defined as

$$\mathbf{q}_d(t) := \begin{bmatrix} q_{1d}(t) \\ \mathbf{q}_{ad}(t) \end{bmatrix} := \mathbf{q}_0(t-T_k), t \in (T_k, T_{k+1}], \quad (6)$$

where $T_0 = t_0 = 0$ and T_k ($k \in \{1,2,...\}$) is the moment of the k^{th} actual landing and $\mathbf{q}_0(t)$ is a smooth extension of $\bar{\mathbf{q}}_d(t)$ from $t \in (0, \tau_1]$ to $t \in (-\infty, +\infty)$.

Assuming that there are no disturbances or modeling errors, input-output linearization is utilized to synthesize a controller. Defining the output functions as

$$\mathbf{y}(t) = \mathbf{q}_a(t) - \mathbf{q}_{ad}(t), \quad (7)$$

one has

$$\ddot{\mathbf{y}}(t) = \ddot{\mathbf{q}}_a(t) - \ddot{\mathbf{q}}_{ad}(t) \quad (8)$$

during each continuous phase. Then, from (1) and (4),

$$\ddot{\mathbf{q}}_a = \mathbf{H}\mathbf{M}^{-1}(\mathbf{B}_u\mathbf{u} - \mathbf{h}), \quad (9)$$

where

$$\mathbf{H} := \begin{bmatrix} 0 & 1 & 0 & 0 & 0 \\ 0 & 0 & 1 & 0 & 0 \\ 0 & 0 & 0 & 1 & 0 \\ 0 & 0 & 0 & 0 & 1 \end{bmatrix}.$$

Substituting (9) into (8), one obtains

$$\ddot{\mathbf{y}} = \mathbf{H}\mathbf{M}^{-1}\mathbf{B}_u\mathbf{u} - (\mathbf{H}\mathbf{M}^{-1}\mathbf{h} + \ddot{\mathbf{q}}_{ad}). \quad (10)$$

Therefore, the control law

$$\mathbf{u} = (\mathbf{H}\mathbf{M}^{-1}\mathbf{B}_u)^{-1}(\mathbf{v} + \mathbf{H}\mathbf{M}^{-1}\mathbf{h} + \ddot{\mathbf{q}}_{ad}) \quad (11)$$

with

$$\mathbf{v} = -\mathbf{K}_P\mathbf{y} - \mathbf{K}_D\dot{\mathbf{y}} \quad (12)$$

results in a linearized system

$$\begin{bmatrix} \dot{\mathbf{y}} \\ \ddot{\mathbf{y}} \end{bmatrix} = \begin{bmatrix} \mathbf{0}_{4\times4} & \mathbf{I}_{4\times4} \\ -\mathbf{K}_P & -\mathbf{K}_D \end{bmatrix} \begin{bmatrix} \mathbf{y} \\ \dot{\mathbf{y}} \end{bmatrix} := \mathbf{A}(\mathbf{K}_P, \mathbf{K}_D) \begin{bmatrix} \mathbf{y} \\ \dot{\mathbf{y}} \end{bmatrix}, \quad (13)$$

where $\mathbf{H}\mathbf{M}^{-1}\mathbf{B}_u$ is supposed to be globally invertible [4], $\mathbf{0}_{4\times4} \in \mathbb{R}^{4\times4}$ is a zero matrix, $\mathbf{I}_{4\times4} \in \mathbb{R}^{4\times4}$ is an identity matrix, and $\mathbf{K}_P \in \mathbb{R}^{4\times4}$ and $\mathbf{K}_D \in \mathbb{R}^{4\times4}$ are positive definite diagonal matrices to be designed. If the proportional-derivative (PD) gains in $\mathbf{K}_P$ and $\mathbf{K}_D$ are chosen such that $\mathbf{A}$ is Hurwitz, then the output functions $\mathbf{y}(t)$ will converge to zero exponentially fast during each continuous phase [14].

Note that the periodic trajectories $\bar{\mathbf{q}}_d(t)$ will need to be first determined before $\mathbf{q}_d(t)$ and $\mathbf{y}(t)$ can be defined. Due to the underactuation, an arbitrary set of periodic functions may not be a solution of the control system in (1), (11) and (12). However, searching of the desired periodic solution $\bar{\mathbf{q}}_d(t)$ will not be discussed here, as the focus of this study is on controller design and stability analysis. In the following section, the stability of $\bar{\mathbf{q}}_d(t)$ as a periodic solution of the closed-loop control system will be examined.

III. Closed-loop Stability Analysis

It is challenging to analyze the stability of a closed-loop system that is hybrid and nonautonomous with internal dynamics and an impulse effect. Also, the stability analysis results should be useful for gait motion planning.

Define the state as:

$$\mathbf{x} := \begin{bmatrix} \mathbf{x}_1 \\ \mathbf{x}_2 \end{bmatrix} := \begin{bmatrix} \mathbf{q} \\ \dot{\mathbf{q}} \end{bmatrix} \in \mathbb{R}^{10}. \quad (14)$$

Accordingly, denote

$$\bar{\mathbf{x}}_d(t) := \begin{bmatrix} \bar{\mathbf{q}}_d(t) \\ \dot{\bar{\mathbf{q}}}_d(t) \end{bmatrix} \in \mathbb{R}^{10} \quad (15)$$

and

$$\mathbf{x}_d(t) := \begin{bmatrix} \mathbf{q}_d(t) \\ \dot{\mathbf{q}}_d(t) \end{bmatrix} \in \mathbb{R}^{10}. \quad (16)$$

From (1), (7), (8), (11), and (12), the closed-loop system can be rewritten as

$$\begin{cases} \dot{\mathbf{x}} = \mathbf{f}(t, \mathbf{x}), & \text{if } \mathbf{x} \notin S(\mathbf{x}); \\ \Delta\mathbf{x} = \mathbf{I}(\mathbf{x}), & \text{if } \mathbf{x} \in S(\mathbf{x}); \end{cases} \quad (17)$$

with the switching surface

$$S(\mathbf{x}) := \{\mathbf{x} \in \mathbb{R}^{10} : \mathrm{h}(\mathbf{x}_1) = 0, \frac{\partial \mathrm{h}}{\partial \mathbf{x}_1}\mathbf{x}_2 < 0\}, \quad (18)$$

where the expression of $\mathbf{I}(\mathbf{x})$ can be derived based on $\mathbf{I}_q(\mathbf{q}, \dot{\mathbf{q}})$ and the expression of

$$\mathbf{f}(t, \mathbf{x}) := \begin{bmatrix} \mathbf{f}_1(t, \mathbf{x}) \\ \mathbf{f}_2(t, \mathbf{x}) \end{bmatrix} \quad (19)$$

is obtained as:

$$\begin{aligned} \mathbf{f}_1(t, \mathbf{x}) :&= \mathbf{x}_2, \\ \mathbf{f}_2(t, \mathbf{x}) :&= [\mathbf{M}^{-1}\mathbf{B}_u(\mathbf{H}\mathbf{M}^{-1}\mathbf{B}_u)^{-1}\mathbf{H} - \mathbf{I}_{5\times5}]\mathbf{M}^{-1}\mathbf{h} \\ &+ \mathbf{M}^{-1}\mathbf{B}_u(\mathbf{H}\mathbf{M}^{-1}\mathbf{B}_u)^{-1}[\ddot{\mathbf{q}}_{ad}(t) - \mathbf{K}_P(\mathbf{H}\mathbf{x}_1 - \mathbf{q}_{ad}(t)) \\ &- \mathbf{K}_D(\mathbf{H}\mathbf{x}_2 - \dot{\mathbf{q}}_{ad}(t))]. \end{aligned} \quad (20)$$

In the following, a new state variable ρ is introduced, and the nonautonomous closed-loop dynamics in (17) will be transformed into an equivalent autonomous system with an augmented set of states. The new state variable ρ is defined as

$$\rho = t - T_k, \quad t \in (T_k, T_{k+1}], \quad (21)$$

during the $(k+1)^{th}$ step ($k \in \{0,1,2,...\}$). By this definition, ρ is reset to zero at the beginning of a step and indicates how long a step has taken. Also, when a biped travels on the desired periodic solution $\bar{\mathbf{x}}_d(t)$, T_k coincides with τ_k for all $k \in \{0,1,2,...\}$, and ρ varies periodically and is denoted as $\bar{\rho}_d(t)$,

$$\bar{\rho}_d(t) = t - \tau_k, \quad t \in (\tau_k, \tau_{k+1}], \tag{22}$$

for $k \in \{0,1,2,...\}$.

From (21), the dynamics associated with ρ can be obtained as:

$$\begin{cases} \dot{\rho} = 1, & \text{if } \mathbf{x} \notin S(\mathbf{x}); \\ \rho^+ = 0, & \text{if } \mathbf{x} \in S(\mathbf{x}). \end{cases} \tag{23}$$

From (6) and (21), one has $\mathbf{q}_d(t) = \mathbf{q}_0(\rho)$, and thus there exists a function $\mathbf{g}(\rho,\mathbf{x})$ that coincides with $\mathbf{f}(t,\mathbf{x})$ during the continuous phases.

Now, define the augmented state $\mathbf{x}_e$ as:

$$\mathbf{x}_e := \begin{bmatrix} \rho \\ \mathbf{x} \end{bmatrix} \in \mathbb{R}^{11}. \tag{24}$$

Correspondingly, denote

$$\bar{\mathbf{x}}_{ed}(t) := \begin{bmatrix} \bar{\rho}_d(t) \\ \bar{\mathbf{x}}_d(t) \end{bmatrix} \in \mathbb{R}^{11}. \tag{25}$$

Then, an autonomous system that is equivalent to (17) can be obtained as

$$\begin{cases} \dot{\mathbf{x}}_e = \mathbf{g}_e(\mathbf{x}_e), & \text{if } \mathbf{x}_e \notin S_e(\mathbf{x}_e); \\ \Delta\mathbf{x}_e = \mathbf{I}_e(\mathbf{x}_e), & \text{if } \mathbf{x}_e \in S_e(\mathbf{x}_e); \end{cases} \tag{26}$$

with

$$S_e(\mathbf{x}_e) := \{\mathbf{x}_e \in \mathbb{R}^{11} : \psi_e(\mathbf{x}_e) = 0, \frac{\partial \psi_e}{\partial \mathbf{x}_e}(\mathbf{x}_e)\mathbf{g}_e(\mathbf{x}_e) < 0\},$$

where

$$\mathbf{g}_e(\mathbf{x}_e) := \begin{bmatrix} 1 \\ \mathbf{g}(\rho,\mathbf{x}) \end{bmatrix}, \ \mathbf{I}_e(\mathbf{x}_e) := \begin{bmatrix} -\rho \\ \mathbf{I}(\mathbf{x}) \end{bmatrix}, \ \psi_e(\mathbf{x}_e) := h(\mathbf{x}_1).$$

Since the original nonautonomous closed-loop system in (17) is equivalent to the autonomous augmented system in (26), the main theorem of closed-loop stability is presented as follows.

Theorem 1: If the following conditions are satisfied:

(A1) $\frac{\partial h}{\partial \mathbf{x}}(\bar{\mathbf{x}}_d(\tau_k))\dot{\bar{\mathbf{x}}}_d(\tau_k) \neq 0$;

(A2) There is no beating at a landing impact;

(A3) The monodromy matrix of the following linear periodically varying system has only one unity-modulus eigenvalue, and the maximum modulus of all the other eigenvalues is strictly less than one:

$$\begin{cases} \frac{d\mathbf{z}}{dt} = \frac{\partial \mathbf{g}_e}{\partial \mathbf{x}_e}(\bar{\mathbf{x}}_{ed}(t))\mathbf{z}, & \text{if } t \neq \tau_k; \\ \Delta\mathbf{z} = \mathbf{M}_k\mathbf{z}, & \text{if } t = \tau_k; \end{cases} \tag{27}$$

where

$$\mathbf{M}_k = \frac{\partial \mathbf{I}_e}{\partial \mathbf{x}_e} + [\mathbf{g}_e^+ - \mathbf{g}_e - \frac{\partial \mathbf{I}_e}{\partial \mathbf{x}_e}\mathbf{g}_e] \frac{\frac{\partial \psi_e}{\partial \mathbf{x}_e}}{\frac{\partial \psi_e}{\partial \mathbf{x}_e}\mathbf{g}_e} \tag{28}$$

and

$$\begin{aligned} \mathbf{g}_e &= \mathbf{g}_e(\bar{\mathbf{x}}_{ed}(\tau_k)), & \mathbf{g}_e^+ &= \mathbf{g}_e(\bar{\mathbf{x}}_{ed}(\tau_k^+)), \\ \frac{\partial \mathbf{I}_e}{\partial \mathbf{x}_e} &= \frac{\partial \mathbf{I}_e}{\partial \mathbf{x}_e}(\bar{\mathbf{x}}_{ed}(\tau_k)), & \frac{\partial \psi_e}{\partial \mathbf{x}_e} &= \frac{\partial \psi_e}{\partial \mathbf{x}_e}(\bar{\mathbf{x}}_{ed}(\tau_k)). \end{aligned} \tag{29}$$

Then, $\bar{\mathbf{x}}_d(t)$ is a locally orbitally exponentially stable solution of the closed-loop system in (17). ■

Skecth of Proof: The linear system in (27) is the variational equation of the augmented autonomous system in (26) [15]. It is straightforward to verify that the biped model in (17) satisfies the following conditions:

1) During the continuous phase of the k^{th} step ($k \in \{1,2,...\}$), the function $\mathbf{f} : \mathbb{R}^+ \times \mathbb{R}^{10} \to \mathbb{R}^{10}$ coincides with the function $\mathbf{f}_k : \mathbb{R}^+ \times \mathbb{R}^{10} \to \mathbb{R}^{10}$ that is continuously differentiable on $\mathbb{R}^+ \times \mathbb{R}^{10}$.
2) The function $\mathbf{I} : \mathbb{R}^{10} \to \mathbb{R}^{10}$ is continuously differentiable on $\mathbb{R}^{10}$;
3) $h : \mathbb{R}^{10} \to \mathbb{R}$ is continuously differentiable on $\mathbb{R}^{10}$.

Then, by Theorem 1 in [15], Condition (A3) guarantees that there exists a positive number $\delta > 0$ such that for any $\mathbf{x}_e(0) \in B_\delta(\Gamma)$, where $\Gamma := \{\mathbf{x}_e \in \mathbb{R}^{11} : \mathbf{x}_e = \bar{\mathbf{x}}_{ed}(t), t \in (0,\tau]\}$, $\mathbf{x}_e(t)$ will converge to the periodic orbit Γ exponentially fast. Because the original system in (17) is equivalent to (26) and by the definition of $\bar{\mathbf{x}}_{ed}$ in (25), $\bar{\mathbf{x}}_d(t)$ is a locally orbitally exponentially stable solution of the original closed-loop system in (17). ■

Conditions (A1) and (A2) are straightforward to verify, but evaluation of Condition (A3) requires numerical computation. Note that the monodromy matrix in Condition (A3) always has an eigenvalue of zero because ρ is reset to zero upon a swing-foot landing. Also, due to the facts that we are dealing with orbital stabilization and that the augmented system in (26) is autonomous, the monodromy matrix in Condition (A3) always has a unity-modulus eigenvalue [16], denoted as λ_1. Thus, the one with the maximum modulus among all the other eigenvalues determines the stability of the desired orbit Γ and is denoted as λ_s.

IV. Simulation Results

In this section, a planar biped with five revolute joints (see Fig. 1) is simulated to show the validity of the proposed time-dependent orbital stabilization.

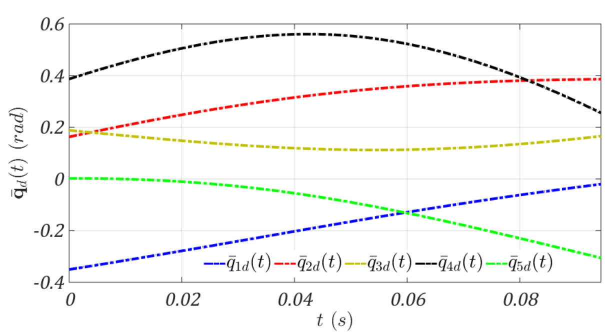

Fig. 3. Desired joint position trajectories $\bar{\mathbf{q}}_d(t)$ during a complete step.

The desired periodic symmetric joint trajectories $\bar{\mathbf{q}}_d(t)$ are obtained through optimization-based motion planning, and the stability conditions in Theorem 1 are included as one of the constraints with the PD gains prespecified as:

$$\mathbf{K}_P = diag(10000, 10000, 10000, 10000);$$

and

$$\mathbf{K}_D = diag(200, 200, 200, 200).$$

Details of motion planning can be found in our related work [17]. The desired joint trajectories $\bar{\mathbf{q}}_d(t)$ are given in Fig. 3.

A. Time-dependent Orbitally Exponential Stabilization

The desired periodic trajectories $\bar{\mathbf{q}}_d(t)$ as shown in Fig. 3 are used to test the proposed controller design and stability conditions. When the PD gains are chosen as $\mathbf{K}_P = diag(10000, 10000, 10000, 10000)$ and $\mathbf{K}_D = diag(200, 200, 200, 200)$, λ_s is computed as $\lambda_s = 0.97 < 1$. Therefore, $\bar{\mathbf{q}}_d(t)$ is an orbitally exponentially stable solution of the closed-loop system under the chosen control gains. Also, from (12), the closed-loop poles associated with the directly controlled joints are all at -100 (rad/s), which is reasonable because the step frequency of $\bar{\mathbf{q}}_d(t)$ is 9.73 (Hz) (i.e., 61 (rad/s)).

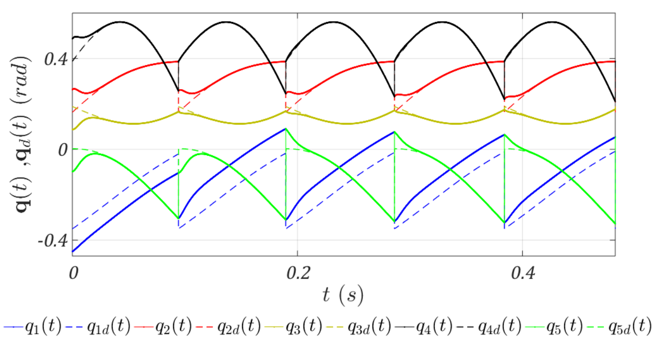

Fig. 4. The actual joint trajectories $\mathbf{q}(t)$ and the desired time functions $\mathbf{q}_d(t)$ during the first 5 steps. Control gains: $\mathbf{K}_P = diag(10000, 10000, 10000, 10000)$; $\mathbf{K}_D = diag(200, 200, 200, 200)$. Initial conditions: $\mathbf{q}(0) - \mathbf{q}_d(0) = \mathbf{q}(0) - \bar{\mathbf{q}}_d(0) = [-0.1, 0.1, -0.1, 0.1, -0.1]^T$; $\dot{\mathbf{q}}(0) - \dot{\mathbf{q}}_d(0) = \dot{\bar{\mathbf{q}}}(0) - \dot{\bar{\mathbf{q}}}_d(0) = [0.1, 0.1, 0.1, 0.1, 0.1]^T$.

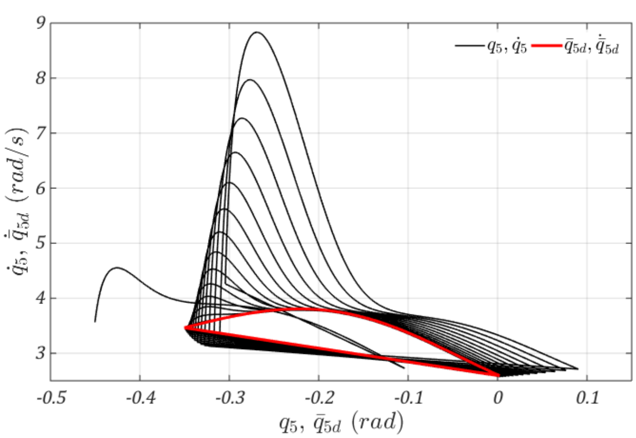

Fig. 5. Exponential convergence of the actual joint trajectories $q_5(t)$ and $\dot{q}_5(t)$ to the desired orbit during the first 15 steps. Control gains: $\mathbf{K}_P = diag(10000, 10000, 10000, 10000)$; $\mathbf{K}_D = diag(200, 200, 200, 200)$. Initial conditions: $\mathbf{q}(0) - \mathbf{q}_d(0) = \mathbf{q}(0) - \bar{\mathbf{q}}_d(0) = [-0.1, 0.1, -0.1, 0.1, -0.1]^T$; $\dot{\mathbf{q}}(0) - \dot{\mathbf{q}}_d(0) = \dot{\bar{\mathbf{q}}}(0) - \dot{\bar{\mathbf{q}}}_d(0) = [0.1, 0.1, 0.1, 0.1, 0.1]^T$.

Simulation results in Fig. 4 show the actual joint trajectories $\mathbf{q}(t)$ and the desired time functions $\mathbf{q}_d(t)$ during 5 steps of underactuated bipedal walking under the proposed time-dependent output feedback control. As shown in Fig. 4, the directly controlled joints $\mathbf{q}_a(t)$ converge to the desired time functions $\mathbf{q}_{ad}(t)$ exponentially fast within each continuous phase, but the unactuated joint $q_1(t)$ does not converge to the desired time function $q_{1d}(t)$ during each continuous phase. However, all of the joints converge to the desired orbit exponentially fast, which is confirmed by the results in Figures 5 and 6. Figure 5 shows the first 15 steps of walking and indicates the exponential convergence of the actual motion to the desired orbit. From Fig. 6, it can be seen that all of the actual joint trajectories exponentially converge to the desired periodic orbit, where the desired joint trajectories $\bar{\mathbf{q}}_d(t)$ reside in, instead of $\bar{\mathbf{q}}_d(t)$ themselves.

B. Effects of PD Control Gains on Closed-loop Stability

The convergence rate of the directly controlled joints $\mathbf{q}_a(t)$ to their desired trajectories $\mathbf{q}_{ad}(t)$ can be adjusted by the PD control gains in $\mathbf{K}_P$ and $\mathbf{K}_D$. Therefore, $\mathbf{K}_P$ and $\mathbf{K}_D$ affect the closed-loop stability. With $\mathbf{K}_P = diag(6400, 6400, 6400, 6400)$ and $\mathbf{K}_D = diag(160, 160, 160, 160)$, λ_s is computed as $\lambda_s = 1.00$, which indicates that the desired periodic trajectories $\bar{\mathbf{q}}_d(t)$ are orbitally stable rather than orbitally exponentially stable. Figure 7 shows the corresponding simulated walking for 20 steps. One can see that the actual joint trajectories in Fig. 7 do not converge to the desired orbit. In fact, they converge to an orbit that is within a small neigborhood of the desired orbit. By comparing the two cases as shown in Fig. 6 and Fig. 7, it is clear that the PD gains indeed affect the closed-loop stability as well as the convergence rate of the actual motion to the desired gait.

V. Conclusions

Orbitally exponential stabilization of underactuated bipedal walking has been studied based on time-dependent output feedback control. Under the assumption that disturbances and modeling errors do not exist, the output feedback linearization method was utilized to synthesize the control law that drives the directly controlled joints to track some desired time functions exponentially fast during each continuous phase. However, the closed-loop stability also depends on the nonautonomous internal dynamics. In order to establish the closed-loop stability conditions, the nonautonomous closed-loop system was equivalently transformed into an augmented autonomous system. Then, the orbitally exponential stability of a periodic solution of the original closed-loop system was evaluated based on the eigenvalues of the monodromy matrix that is associated with the variational equations of the augmented system. Simulation results showed that the proposed walking strategy can effectively guarantee exponential tracking of the desired orbit and that the design parameters of the output feedback controller affect the closed-loop stability.

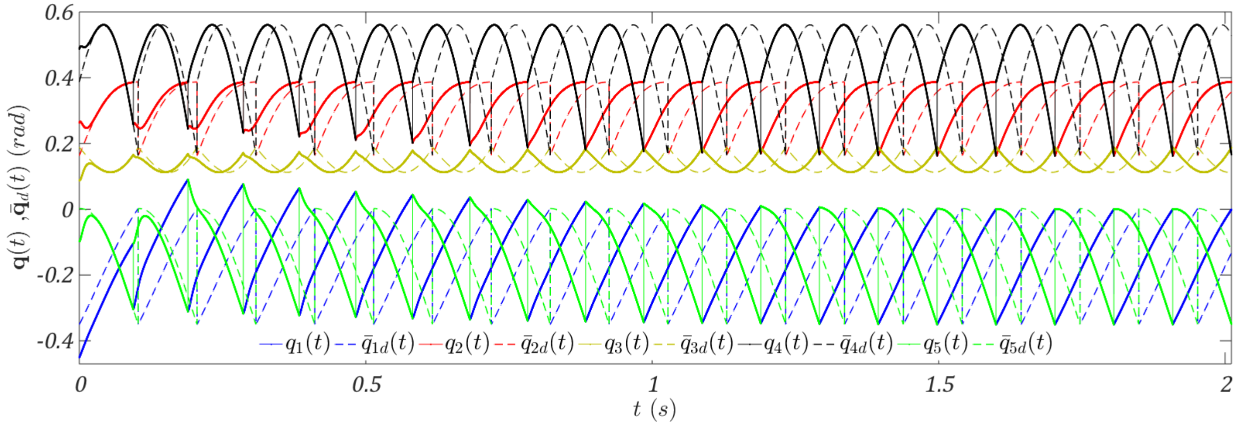

Fig. 6. The actual joint trajectories $\mathbf{q}(t)$ and the desired periodic symmetric joint trajectories $\bar{q}_d(t)$ during the first 20 steps. Control gains: $\mathbf{K}_P = diag(10000, 10000, 10000, 10000)$; $\mathbf{K}_D = diag(200, 200, 200, 200)$. Initial conditions: $\mathbf{q}(0) - \mathbf{q}_d(0) = \mathbf{q}(0) - \bar{\mathbf{q}}_d(0) = [-0.1, 0.1, -0.1, 0.1, -0.1]^T$; $\dot{\mathbf{q}}(0) - \dot{\mathbf{q}}_d(0) = \dot{\bar{\mathbf{q}}}(0) - \dot{\bar{\mathbf{q}}}_d(0) = [0.1, 0.1, 0.1, 0.1, 0.1]^T$.

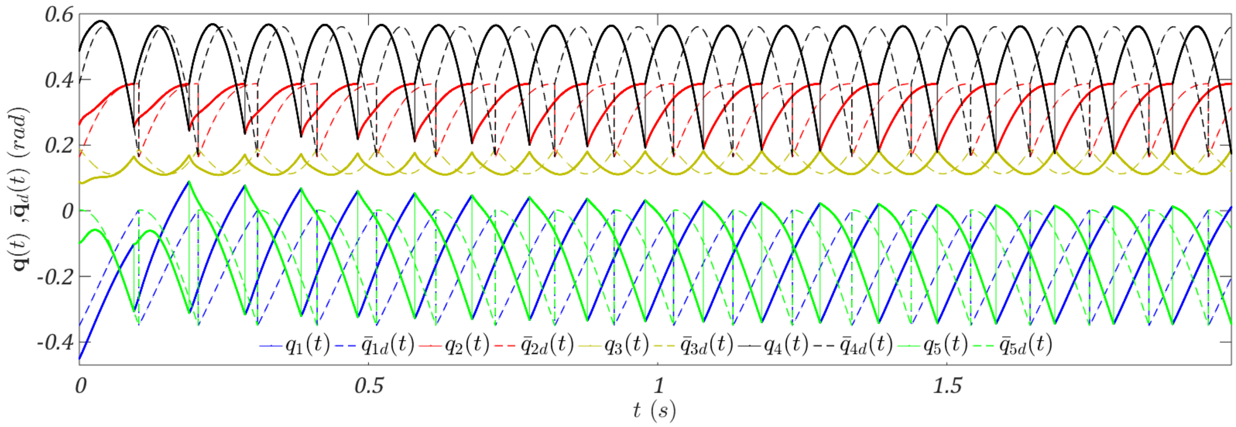

Fig. 7. The actual joint trajectories $\mathbf{q}(t)$ and the desired periodic symmetric joint trajectories $\bar{q}_d(t)$ during the first 20 steps. Control gains: $\mathbf{K}_P = diag(6400, 6400, 6400, 6400)$; $\mathbf{K}_D = diag(160, 160, 160, 160)$. Initial conditions: $\mathbf{q}(0) - \mathbf{q}_d(0) = \mathbf{q}(0) - \bar{\mathbf{q}}_d(0) = [-0.1, 0.1, -0.1, 0.1, -0.1]^T$; $\dot{\mathbf{q}}(0) - \dot{\mathbf{q}}_d(0) = \dot{\bar{\mathbf{q}}}(0) - \dot{\bar{\mathbf{q}}}_d(0) = [0.1, 0.1, 0.1, 0.1, 0.1]^T$.

References

[1] M. Vukobratovic, A. A. Frank, and D. Juricic, "On the stability of biped locomotion," *IEEE Transactions on Bio-Medical Engineering*, vol. 17, no. 1, pp. 25–26, 1970.

[2] M. Vukobratović and B. Borovac, "Zero-moment point–thirty five years of its life," *International Journal of Humanoid Robotics*, vol. 1, no. 01, pp. 157–173, 2004.

[3] S. Kajita, F. Kanehiro, K. Kaneko, K. Fujiwara, K. Harada, K. Yokoi, and H. Hirukawa, "Biped walking pattern generation by using preview control of zero-moment point," in *Proc. of IEEE International Conference on Robotics and Automation*, 2003, pp. 1620–1626.

[4] J. Grizzle, G. Abba, and P. Plestan, "Asymptotically stable walking for biped robots: Analysis via systems with impulse effects," *IEEE Transactions on Automatic Control*, vol. 46, no. 1, pp. 51–64, 2001.

[5] J. W. Grizzle, C. Chevallereau, R. W. Sinnet, and A. D. Ames, "Models, feedback control, and open problems of 3D bipedal robotic walking," *Automatica*, vol. 50, no. 8, pp. 1955–1988, 2014.

[6] B. Griffin and J. Grizzle, "Nonholonomic virtual constraints for dynamic walking," in *Proc. of IEEE Conference on Decision and Control*, 2015, pp. 4053–4060.

[7] X. Da, O. Harib, R. Hartley, B. Griffin, and J. W. Grizzle, "From 2D design of underactuated bipedal gaits to 3D implementation: Walking with speed tracking," *IEEE Access*, vol. 4, pp. 3469–3478, 2016.

[8] E. R. Westervelt, J. W. Grizzle, and D. E. Koditschek, "Hybrid zero dynamics of planar biped walkers," *IEEE Transactions on Automatic Control*, vol. 48, no. 1, pp. 42–56, 2003.

[9] B. Morris and J. W. Grizzle, "Hybrid invariant manifolds in systems with impulse effects with application to periodic locomotion in bipedal robots," *IEEE Transactions on Automatic Control*, vol. 54, no. 8, pp. 1751–1764, 2009.

[10] S. Kolathaya, A. Hereid, and A. D. Ames, "Time dependent control lyapunov functions and hybrid zero dynamics for stable robotic locomotion," in *Proc. of American Control Conference*, 2016, pp. 3916–3921.

[11] T. Wang and C. Chevallereau, "Stability analysis and time-varying walking control for an under-actuated planar biped robot," *Robotics and Autonomous Systems*, vol. 59, no. 6, pp. 444–456, 2011.

[12] J. W. Grizzle, A. Gabriel, and P. Franck, "Proving asymptotic stability of a walking cycle for a five dof biped robot model," in *Proc. of International Conference on Climbing and Walking Robots*, 1999, pp. 4048–4053.

[13] Y. Gu, B. Yao, and C. S. G. Lee, "Bipedal gait recharacterization and walking encoding generalization for stable dynamic walking," in *Proc. of IEEE International Conference on Robotics and Automation*, 2016, pp. 1788–1793.

[14] H. K. Khalil, *Nonlinear control*. Prentice Hall, 1996.

[15] P. S. Simeonov and D. D. Bainov, "Exponential stability of the solutions of the initial-value problem for systems with impulse effect," *Journal of Computational and Applied Mathematics*, vol. 23, no. 3, pp. 353–365, 1988.

[16] D. Bainov and P. Simeonov, *Impulsive differential equations: periodic solutions and applications*. CRC Press, 1993.

[17] Y. Gu, B. Yao, and C. S. G. Lee, "Output function optimization for stable underactuated bipedal walking," in *Proc. of 2017 IFAC World Congress*, to appear.